International Workshop on Stellar Spectral Libraries
ASI Conference Series, 2014, Vol. 11, pp 25 – 32
Editors: H. P. Singh, P. Prugniel and I. Vauglin

The X-shooter Spectral Library (XSL) in the near-infrared: Case study of carbon stars

A. Gonneau[1,2*], A. Lançon[1], S. C. Trager[2], Y. P. Chen[2],
R. Peletier[2], B. Aringer[3,4] and W. Nowotny[4]
[1]*Observatoire Astronomique de Strasbourg, Université de Strasbourg, CNRS, UMR 7550, 11 rue de l'Université, F-67000 Strasbourg, France*
[2]*Kapteyn Astronomical Institute, University of Groningen, Postbus 800, 9700 AV, Groningen, Netherlands*
[3]*Dipartimiento di Astronomica, Università di Padova, Vicolo dell'Osservatorio 2, 35122 Padova, Italy*
[4]*University of Vienna, Department of Astrophysics, Türkenschanzstraße 17, A-1180 Wien, Austria*

Abstract. The X-shooter Spectral Library (XSL) is a new stellar spectral library, aiming at improving the spectral population synthesis models. This paper focuses on XSL spectra of carbon stars, which are key elements for population synthesis. A comparison with theoretical spectra is necessary to estimate the fundamental parameters of the observed stars, as well as to validate the spectral models across the broad ultraviolet to near-infrared wavelength range of X-shooter. We present the results of such comparisons.

Keywords : spectroscopy, instrument: X-shooter, wavelength: near-infrared, stars: carbon

1. Introduction

Spectral population synthesis models are powerful tools for the study of galaxies, but they rely on libraries of stellar spectra. The ideal library would cover a large range of stellar parameters (in effective temperature, surface gravity and metallicity) and have an extended wavelength coverage. Galaxy light comes predominately from stellar

*email: anais.gonneau@astro.unistra.fr

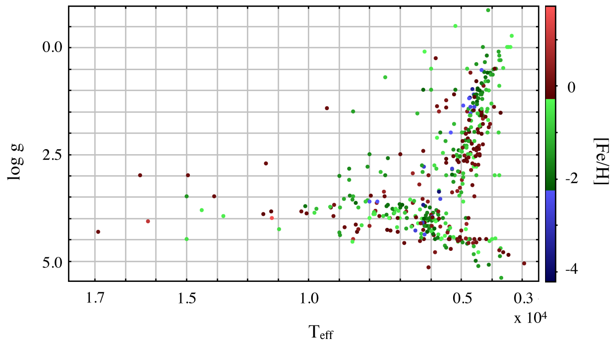

Figure 1. Early XSL sample. Only 436 stars are displayed here.

photospheres across near-ultraviolet, visible and near-infrared wavelengths. Unfortunately, there is no empirical library covering all these parts of the spectrum at the same time, with a resolution and a number of stars comparable to the ones existing for the optical.

The X-shooter Spectral Library (XSL, Chen et al. 2011) is intended to meet this need. Thanks to an ESO Large Programme and making use of X-shooter's unique capability (see Vernet et al. 2011), our stellar library will consist of about 700 stars, observed at moderate resolution (R ∼ 10 000), with complete coverage from 320 to 2480 nm, covering a large range of stellar parameters (log g, Teff, [Fe/H]), as shown in Fig. 1.

In order to feed population synthesis models adequately, we aimed to sample the full range of relevant spectral types. To do so, we selected stars from Lick/IDS (Worthey and Ottaviani 1997), MILES (Sáncez-Blázquez et al. 2006) and NGSL (Gregg et al. 2006). In addition, we added red giant branch stars from the disk, the bulge and from stellar clusters, asymptotic giant stars from the Milky Way (MW), the Large Magellanic Cloud (LMC) and the Small Magellanic Cloud (SMC), and red supergiants stars from the MW, the LMC and the SMC.

Among the variety of stars in XSL, this presentation focuses on one spectral type: the carbon stars. Carbon stars are among the brightest stellar objects in resolved galaxies containing young and intermediate age populations, mainly radiating in the near-infrared. In addition, they contribute significantly to the integrated spectra of such systems. Up to now, only two libraries contain C-stars: IRTF-Spex (Rayner et al. 2009) and Lançon and Wood (2000). So, there is a real need of larger spectral libraries of C-rich stars with a range of metallicities before being able to reproduce their contribution to the stellar population models, as highlighted by Luybenova et al. (2012).

The X-shooter Spectral Library is intended to contain up to 40 carbon stars. Before the end of this Large Programme, we can use the subset of C-star spectra already acquired to tackle the following question: can the observed spectra across the whole wavelength range (visible to near-infrared) be reproduced with synthetic spectra? Answering this question is an essential step towards establishing the evolutionary status of the observed stars, which is necessary for population synthesis purposes. Section 2 will introduce the very basis of our reduction process. In Section 3, we will present the models we are using for this comparison. Then, in Sections 4 and 5, we will present early results of this discussion.

2. Data reduction process in the near-infrared

In this section, we give a brief description of the data reduction process in the near-infrared. More details can be found in a forthcoming paper.

The data reduction for the near-infrared part of the spectrum follows roughly the same steps as for the UVB/VIS parts (see Chen et al., in preparation). One of the main difference is the correction of the telluric absorption lines. Indeed, the near-infrared is more affected by molecular absorption bands of the atmosphere than the rest of the spectrum. For the near-infrared, we used telluric transmission models provided by ESO, in collaboration with the University of Innsbruck (see Moehler et al., in preparation).

The reduction steps can be summarized as follows:

- Reduction with the X-shooter pipeline (version 2.2.0)
- Extraction of the 1D spectra from the rectified, wavelength calibrated 2D images with Iraf
- Telluric-correction and flux-calibration procedure

To correct our spectra from the telluric absorption, we perform a Principal Component Analysis on a subset of telluric transmission models. Thanks to this, we build a "best" telluric model and divide our observation by it.

Fig. 2 displays an example of the data reduction process for the near-infrared. The upper spectrum is a carbon star spectrum reduced with the pipeline and extracted with Iraf. The bottom spectrum is the same spectrum, corrected for the telluric absorption lines and flux calibrated. The grey areas mask the regions where the telluric correction goes to 0 (in the upper spectrum or in the model), and thus no reconstruction is possible. The middle spectrum is a telluric model, with an airmass close to the one of the observed spectrum, not smoothed yet to the resolution of our observations.

Fig. 3 shows some examples of near-infrared carbon star spectra, reduced and flux calibrated. The two panels correspond to two different populations, respectively the Small Magellanic Cloud (SMC) for the left panel, and the Milky Way (MW) for

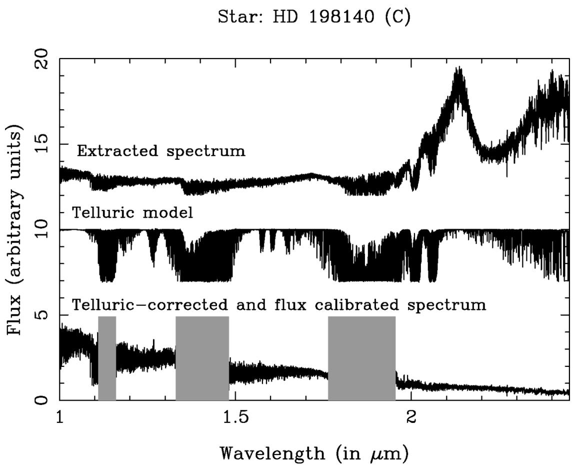

Figure 2. Example of the data reduction process for the near-infrared. The upper spectrum is a 1D carbon star spectrum. The bottom spectrum is the same spectrum, after correction for the telluric absorption lines and flux calibration. The grey areas mask the regions of deepest telluric absorption. The middle spectrum is a telluric model, before smoothing.

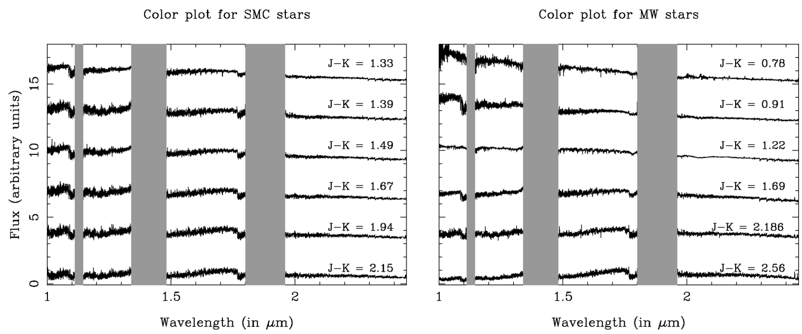

Figure 3. Left: Examples of NIR C-star spectra from the Small Magellanic Cloud. **Right:** Examples of NIR C-star spectra from the Milky Way.

the right panel. On each panel, the spectra are ordered by decreasing (J-K). We can see that for the SMC, molecular features can remain remarkably similar over a broad range in color. The two top spectra however illustrate how, at similar (J-K), the C/O ratio affects the relative strengths of bands of CO, CN and C_2. The MW subsample displays a larger variety.

3. Models

The set of models used for this study are the model atmospheres of C-rich giants calculated by Aringer et al. (2009). These authors computed a grid of 746 spherically symmetric COMARCS atmospheres covering effective temperatures between 2400 and 4000 K, surface gravities from log(g[cm/s^2]) = 0.0 to −1.0, metallicities ranging from the solar value down to one-tenth solar and C/O ratios in the interval between 1.05 and 5.0. For the present study, only log (g[cm/s^2]) = 0.0, and solar metallicity were used. We computed for our need new synthetic spectra at high resolution (R = 200000), that we smoothed afterwards to match the resolution of XSL data.

Aringer et al. show that their hydrostatic models reproduce the colors of the warmer carbon stars with weak pulsation. But to deal with cooler objects with intense variations, a proper treatment of the reddening caused by dusty envelopes is needed. Thus, more sophisticated model atmospheres are needed to deal with more evolved C-rich red giants for which dynamic phenomena (pulsation and developments of dusty stellar winds) become significant, as demonstrated by Nowotny et al. (2011) and Nowotny et al. (2013).

In our study, we choose to first compare our observations with the models developed by Aringer et al. (2009), as a first guess, before working with the dynamical models. To take into account the reddening due to circumstellar dust which is not included in the static models, we used a set of parameterized extinction laws (Cardelli et al. (1989); R_V = 3.1 is used here, but this constraint will be relaxed). To determine our best fits, we perfom a χ^2 minimization in a three-dimensional space: effective temperature, C/O ratio and the visual extinction A_V.

4. Best fits to NIR observations

In the following section, we will show some examples of our best fits to NIR observations. The first aim of comparing our observations with models is to give estimates of the fundamental stellar parameters, such as the effective temperature and the C/O ratio.

The first star under study here is 2MASS-J00493262 (Simbad name: RAW 553), with (J-K) = 1.43. The parameters found are: Teff = 3 600 K, C/O = 1.1 and A_V = 1.9. Fig. 4 displays the best fit for 2MASS-J00493262. The two panels are computed at two different resolutions. The upper panel shows the result of the best fit for the whole near-infrared spectrum, then smoothed to R ~ 2 300 for display purpose. The bottom panel shows a zoom of the best fit around 1.1 μm at the initial X-shooter resolution for NIR (R ~8 000). The agreement between the model and the observation is quite good, although some systematic differences remain to be explained.

The second star shown is HD 198140, with (J-K) = 0.9. The parameters found are: Teff = 4 000 K, C/O = 1.4 and A_V = 0.1. Fig. 5 displays the best fit for HD 198140. In that case also, the model provides a good first order representation of the spectrum in the near-infrared arm. Uncertainties on the stellar parameters related to Teff-Av and Teff - C/O degeneracies remain to be quantified.

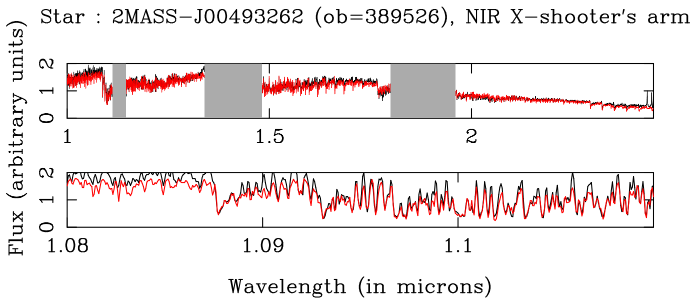

Figure 4. Best fit (red) to the XSL-NIR spectrum (black) of a C-star ((J-K) = 1.43). The grey bands mask the regions of deepest telluric absorption. The upper panel shows the spectra smoothed to R ~ 2 300, while the lower is a zoom at R ~ 8 000.

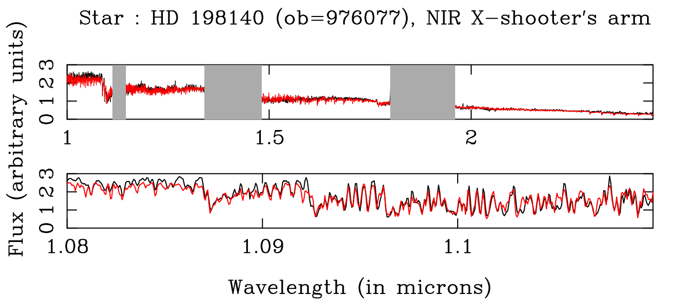

Figure 5. Best fit (red) to the XSL-NIR spectrum (black) of a C-star ((J-K) = 0.9). The grey bands mask the regions of deepest telluric absorption. The upper panel shows the spectra smoothed to R ~ 2 300, while the lower is a zoom at R ~ 8 000.

5. Extension to the visible

As shown in section 4, there is a promising agreement in the near-infrared between models and observations. Making use of X-shooter's wavelength range, we investigate simultaneously the visible and the near-infrared parts of the spectrum.

The first test we perform is a χ^2 minimization on the visible part of the spectrum of HD 198140. The parameters found are in total agreement with the ones found for the NIR: Teff = 4 000 K, C/O = 1.4 and A_V = 0.1. Fig. 6 displays the result. The upper panel shows the best fit (red curve) to VIS observation (black curve), while the bottom panel shows the best fit (red curve) to NIR observation.

Another interesting test is to extend the results found in the near-infrared part of

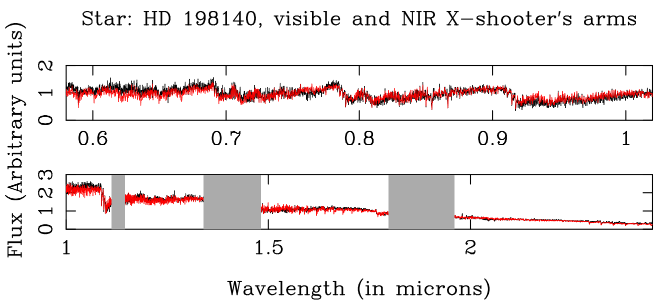

Figure 6. Best fit (red) to the XSL VIS-NIR spectrum (black) of a C-star ((J-K) = 0.9). The grey bands mask the regions of deepest telluric absorption. The upper panel shows the VIS fitting, and the lower one the NIR fitting. Synthetic and observed spectra are rebinned to R ∼ 2300.

the spectrum to the visible. The star under study is RAW 1033 ((J-K) = 1.5). Fig. 7 displays the result. The red curve is our best fit, extended to the visible, and the black curve is the merged empirical spectrum. In the visible, some deviations appear, which are not due to the flux calibration. Tests performed with other C-stars indicate that bluer stars (for which the circumstellar reddening is less pronounced) are more easily reproduced. In addition, as mentioned by Nowotny et al. (2011), parameters for observed C-star derived from studies based on hydrostatic models should be regarded with caution.

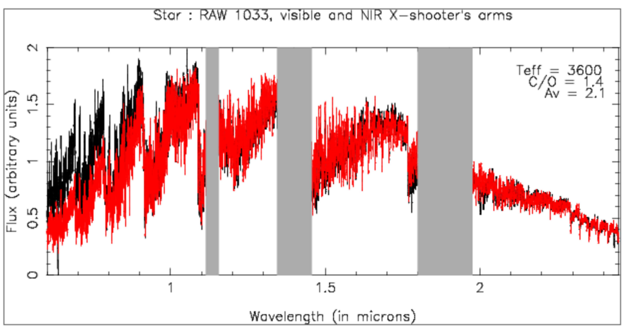

Figure 7. Best fit (red) to the XSL-NIR spectrum, extended to the visible, and the merged empirical spectrum (black curve). Synthetic and observed spectra are rebinned to R ∼ 2300. The grey bands mask the regions of deepest telluric absorption.

6. Conclusions

New facilities, such as the E-ELT or the JWST, are coming, with an enhanced sensivity in the infrared. Thus, developing stellar population tools in the near-infrared is more than needed. The X-shooter Spectral Library will be a starting point. XSL provides a large collection of stellar spectra, with moderate resolution, broad wavelength coverage and large range of stellar atmospheric parameters. Among this collection, carbon stars are key elements for the stellar population synthesis applications. Therefore, a proper determination of their fundamental parameters is crucial. While comparing our observed carbon spectra to hydrostatic models, reddened with a standard extinction law, we find a good agreement between both spectra. This is no longer the case when we investigate the whole visible-near-infrared spectrum. The next step is now to work with the dynamical models, keeping in mind the final objective: improving the robustness of fundamental parameter estimates for population synthesis uses.

Acknowledgements

A. Gonneau would like to thank the organizers for this conference, and her colleagues for helpful discussions. XSL is based on ESO Large Programme 189.B-0925. This research was funded in part by the Austrian Science Fund (FWF): P21988-N16.

References

Aringer B., Girardi L., Nowotny W., et al., 2009, A&A, 503, 913
Cardelli J. A., Clayton G. C., Mathis J. S., 1989, ApJ, 345, 245
Chen Y. P., Trager S. C., Peletier R., et al., 2011, JPhSC, 328a, 2023
Gregg M. D., Silva D., Rayner J., et al., 2006, The 2005 HST calibration workshop
Lançon A., Wood P. R., 2000, A&AS, 146, 217
Lyubenova M., Kuntschner H., Rejkuba M., et al., 2012, A&A, 543, A75
Nowotny W., Aringer B., Höfner S., et al., 2011, A&A, 529, A129
Nowotny W., Aringer B., Höfner S., et al., 2013, A&A, 552, A20
Rayner J. T., Cushing M. C., Vacca W. D., 2009, ApJS, 185, 289
Sáncez-Blázquez P., Peletier R. F., Jiménez-Vicente J., et al., 2006, MNRAS, 371, 703
Vernet J. et al., 2011, A&A, 536, A105
Worthey G., Ottaviani D. L., 1997, ApJS, 111, 377